

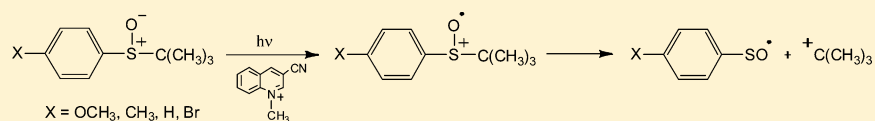
Structural Effects on the C–S Bond Cleavage in Aryl *tert*-Butyl Sulfoxide Radical Cations

Tullio Cavattoni,[†] Tiziana Del Giacco,^{*,‡} Osvaldo Lanzalunga,^{*,†} Marco Mazzonna,[†] and Paolo Mencarelli^{*,†}

[†]Dipartimento di Chimica and Istituto CNR di Metodologie Chimiche-IMC, Sezione Meccanismi di Reazione c/o Dipartimento di Chimica, Sapienza Università di Roma, P.le A. Moro 5, 00185 Rome, Italy

[‡]Dipartimento di Chimica and Centro di Eccellenza Materiali Innovativi Nanostrutturati, Università di Perugia, via Elce di Sotto 8, 06123 Perugia, Italy

Supporting Information



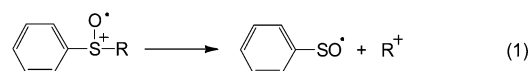
ABSTRACT: The oxidation of a series of aryl *tert*-butyl sulfoxides (4-*X*-C₆H₄SOC(CH₃)₃; **1**, X = OCH₃; **2**, X = CH₃; **3**, X = H; **4**, X = Br) photosensitized by 3-cyano-*N*-methylquinolinium perchlorate (3-CN-NMQ⁺) has been investigated by steady-state irradiation and nanosecond laser flash photolysis (LFP) under nitrogen in MeCN. Products deriving from the C–S bond cleavage in the radical cations **1**^{•+}–**4**^{•+} have been observed in the steady-state photolysis experiments. By laser irradiation, the formation of 3-CN-NMQ[•] ($\lambda_{\text{max}} = 390$ nm) and **1**^{•+}–**4**^{•+} ($\lambda_{\text{max}} = 500$ – 620 nm) was observed. A first-order decay of the sulfoxide radical cations, attributable to C–S bond cleavage, was observed with fragmentation rate constants (k_f) that decrease by increasing the electron donating power of the arylsulfinyl substituent from 1.8×10^6 s⁻¹ (**4**^{•+}) to 2.3×10^5 s⁻¹ (**1**^{•+}). DFT calculations showed that a significant fraction of the charge is delocalized in the *tert*-butyl group of the radical cations, thus explaining the small substituent effect on the C–S bond cleavage rate constants. Via application of the Marcus equation to the kinetic data, a very large value for the reorganization energy ($\lambda = 62$ kcal mol⁻¹) has been calculated for the C–S bond scission reaction in **1**^{•+}–**4**^{•+}.

INTRODUCTION

The chemistry of sulfoxides has attracted continuous interest for its relevance in organic synthesis;¹ moreover, sulfoxide functional groups are present in a number of biologically active molecules and are often involved in the metabolism of sulfides.² One-electron oxidation of sulfoxides represents one of the reactivity aspects of these species that is still little investigated as a consequence of the relatively high oxidation potential of these species.³ Thus, only few studies are presently available for the reactive intermediates produced in this process, that is, sulfoxide radical cations.⁴

In recent years, our group investigated some aspects concerning the structure and reactivity of aromatic sulfoxide radical cations.^{5–8} In particular, we have focused our attention on the C–S bond fragmentation process that represents one of the major decomposition pathways available for both aromatic sulfoxide^{7,8} and aromatic sulfide⁹ radical cations.

The analysis of the fragmentation reactions of tertiary and secondary alkyl phenyl sulfoxide radical cations generated by TiO₂ photocatalyzed⁷ or 3-cyano-*N*-methylquinolinium perchlorate (3-CN-NMQ⁺) photosensitized oxidation⁸ indicates that the heterolytic C–S bond cleavage, leading to the phenylsulfinyl radical C₆H₅SO[•] and the alkyl carbocation R⁺ (eq 1), is a unimolecular process characterized by very high fragmentation rate constants. Interestingly, we found that the



rates of C–S bond cleavage in aromatic sulfoxide radical cations are at least 2 orders of magnitude higher than those observed for the same process occurring in the corresponding sulfide radical cations.^{8,10} This result is in accordance with the significantly higher oxidation potentials of sulfoxides^{5,11} and with the higher stability of the phenylsulfinyl radical with respect to the phenylthiyl radical.¹²

The effect of the structure of the alkyl group on the rate of C–S bond cleavage has been analyzed in detail by steady-state and laser photolysis studies of a series of alkyl phenyl sulfoxide radical cations (in eq 1, R = PhCH₂, Ph(CH₃)CH, Ph₂CH, Ph(CH₃)₂C, or (CH₃)₃C).⁸ It was found that the rates of C–S bond cleavage were very sensitive to the structure of the alkyl group and the strength of the C–S bond in the radical cation, increasing with the stability of the carbocation formed.

More recently, we have investigated in detail the C–S fragmentation process of aryl triphenylmethyl sulfide radical cations. A significant variation of the C–S bond cleavage rates was observed by changing the arylsulfinyl ring substituent.¹³ In

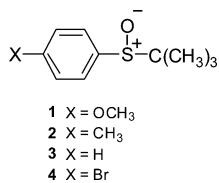
Received: March 4, 2013

Published: April 14, 2013

this context, it has to be noted that previous theoretical studies carried out with a series of aryl-substituted thioanisole radical cations (in 4-X-C₆H₄-SCH₃^{•+}, X = H, CN, OMe, or N(CH₃)₂) showed remarkable differences in the charge and spin distribution on the aromatic ring depending on the nature of the substituent.¹⁴

Along this line, we considered it worthwhile to extend the analysis of the structural effects on the C–S bond cleavage in radical cations of aromatic sulfoxides by changing the substituents in the arylsulfinyl ring, taking into account that also in this case previous theoretical studies performed on aryl methyl sulfoxide radical cations⁵ reported a remarkable effect of the aryl substituent on the charge and spin delocalization. In particular, it was found that in all the radical cations most of the charge and spin density are localized on the SOMe group, but a substantial delocalization was also observed on the aromatic ring (almost 50% for the methoxy derivative and 30% for the other radical cations).

In order to analyze how the electronic effect of the aryl substituents is reflected in the reactivity (C–S fragmentation process) of *tert*-alkyl aryl sulfoxide radical cations, we have carried out a steady-state and laser photolysis study of a series of aryl *tert*-butyl sulfoxides (1–4) in the presence of 3-cyano-*N*-methylquinolinium perchlorate (3-CN-NMQ⁺ClO₄⁻) as a sensitizer in MeCN.^{8,15} We have chosen this class of sulfoxides because the aryl triphenylmethyl sulfoxide radical cations, which would represent a better comparison with the corresponding sulfides, are not stable species and display a reactivity too high to be investigated.



DFT calculations at the B3P86/6-311+G(d,p) level of theory for sulfoxides 1–4 have been carried out to provide us the C–S bond dissociation energy values (BDEs) that have been used to determine the bond dissociation free energies (BDFEs) in the corresponding radical cations 1^{•+}–4^{•+}. DFT calculations at the B3LYP/6-311G(d,p) level of theory have been also carried out in order to obtain information about the geometry, charge, and spin distribution of the radical cations and of the transition states for the C–S bond cleavage process.

RESULTS

Steady-State Photolysis. Steady-state photolysis experiments were carried out by irradiating a solution of sulfoxides 1–4 (1 × 10⁻² M) in N₂-saturated CD₃CN at around 355 nm in the presence of 3-CN-NMQ⁺ClO₄⁻ (1 × 10⁻³ M). The products were identified and quantitated by ¹H NMR (products

from the alkyl moiety) analysis, by HPLC (sulfur containing products) analysis, and by comparison with authentic specimens (¹H NMR spectrum and HPLC chromatogram of the 3-CN-NMQ⁺ photosensitized oxidation of *tert*-butyl 4-methoxyphenyl sulfoxide (1) are reported in the Supporting Information). No products were detected without irradiation or in the absence of the sensitizer.

As reported in the previous study of the oxidation of 3,⁸ the photolysis of sulfoxides 1–4 produced *tert*-butyl alcohol and *tert*-butyl acetamide as reaction products from the *tert*-butyl group and diaryl disulfide (ArSSAr), aryl arenethiosulfinate (ArSOSAr), and aryl arenethiosulfonate (ArSO₂SAr) as sulfur containing fragmentation products (Scheme 1). Small amounts of aryl *tert*-butyl sulfones were also formed.¹⁶ The yields of fragmentation products, referring to the initial amount of substrate, are reported in Table 1.

The total yields exceed the value expected on the basis of the 3-CN-NMQ⁺ amount; thus, the sensitizer is regenerated during the photolysis. Accordingly, UV and ¹H NMR analysis of the reaction mixtures after photolysis indicated that less than 20% of the initial amount of the sensitizer is consumed during the irradiation.

Laser Flash Photolysis Studies. The laser photolysis experiments (λ_{exc} = 355 nm) were performed under nitrogen in the presence of 1 M toluene as a cosensitizer in order to increase the yields of radical cation.¹⁷ Under these conditions, the radical cation of the cosensitizer, PhCH₃^{•+}, is first formed and is able to oxidize the sulfoxide to the corresponding radical cation (E_{red}(PhCH₃^{•+}) = 2.35 V vs SCE).¹⁸ In the LFP experiments with sulfoxides 1, 2, and 4, three main absorption bands were detected just after the laser pulse at 360–400, 450–530, and 550–700 nm. Only the first two absorption bands were observed in the LFP experiments with sulfoxide 3, as has already been reported in a previous study.⁸ As an example, the time-resolved spectra of the LFP experiment with the 3-CN-NMQ⁺/toluene/1 system are reported in Figure 1. Time-resolved spectra for the 3-CN-NMQ⁺/toluene/2 and 3-CN-NMQ⁺/toluene/4 systems are shown in Figures S4 and S5 in the Supporting Information, respectively.

The more stable transient absorption band at around 380 nm can be assigned to the radical 3-CN-NMQ[•] formed after the electron transfer from sulfoxides 1–4 to 3-CN-NMQ^{•+}.⁸

The other two absorption bands can be assigned to the radical cation of the sulfoxides.^{5,8} It is interesting to note that the absorption spectra of the radical cations 1^{•+}, 2^{•+}, and 4^{•+} are different from those of the corresponding aryl methyl sulfoxide radical cations⁵ where only one band was observed significantly red-shifted with respect to the long wavelength absorption band of 1^{•+}, 2^{•+}, and 4^{•+}.

The ΔA recorded at 450–500 nm showed a fast decay of the radical cations, followed by a slower decay which should be assigned to the decay of the radical ArSO[•] that absorbs at these

Scheme 1

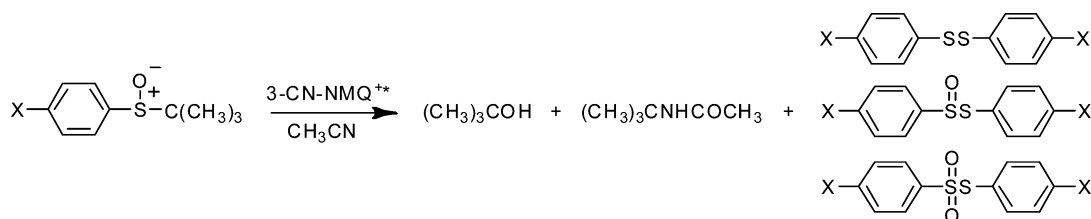
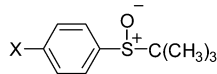


Table 1. C–S Fragmentation Products and Yields in the 3-CN-NMQ⁺ Photosensitized Oxidation of Alkyl Phenyl Sulfoxides (1–4) in N₂-Saturated CD₃CN^a

	Products (Yields %) ^b				
	<i>t</i> BuOH	<i>t</i> BuNHCOCH ₃	ArSSAr	ArSOSAr	ArSO ₂ SAr
1 (X=OCH ₃)	10	19	3	6	4
2 (X=CH ₃)	12	26	4	8	5
3 (X=H)	13	28	6	9	5
4 (X=Br)	21	32	8	10	6

^a[Sulfoxide] = 1.0 × 10⁻² M; [3-CN-NMQ⁺] = 1.0 × 10⁻³ M. ^bYields refer to the initial amount of substrate. The error is ±5%.

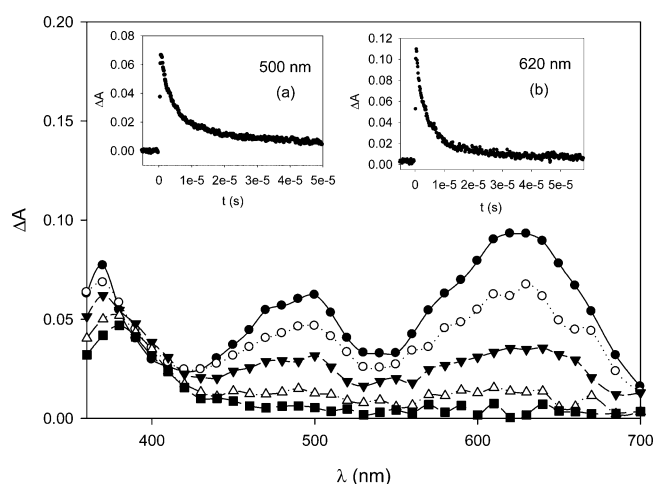


Figure 1. Time-resolved absorption spectra of the 3-CN-NMQ⁺ (8.0 × 10⁻⁴ M)/4-CH₃OC₆H₄SOC(CH₃)₃ (**1**) (1.0 × 10⁻² M) system in N₂-saturated CH₃CN recorded 0.79 (●), 2.1 (○), 5.0 (▼), 32 (△), and 50 (■) μs after the laser pulse. Inset: (a) decay kinetics recorded at 500 nm, and (b) decay kinetics recorded at 620 nm.

wavelengths (see insets of Figure 1 and Figures S4 and S5 in the Supporting Information).¹⁹ The two consecutive decays are more evident with 3^{•+} and 4^{•+} because the decay of the radical cations occurs at a rate much faster than the rate of recombination of ArSO[•].²⁰

In conclusion, LFP experiments confirm the results of the steady-state photolysis, suggesting that the decay of 1^{•+}–4^{•+} is due to the C–S bond cleavage with formation of the *tert*-butyl cation and the arylsulfinyl radicals ArSO[•].

The rates of fragmentation of the aryl *tert*-butyl sulfoxide radical cations 1^{•+}–4^{•+} (*k_f*) were determined by following the

decay kinetics at the λ_{max} of the radical cations (Table 2). In all cases, the decay kinetics followed first-order laws in accordance with a unimolecular fragmentation process. Given the high fragmentation rates, back electron transfer should not be a problem with aryl *tert*-butyl sulfoxide radical cations, as was previously reported for aryl sulfide radical cations.²¹ All the rate constants measured in CH₃CN at 25 °C are reported in Table 2.

Theoretical Calculations. Neutral Sulfoxides. For a meaningful discussion of the experimental results, it was necessary to know the C–S bond dissociation free energies (BDFEs) for the aryl *tert*-butyl sulfoxide radical cations 1^{•+}, 2^{•+}, and 4^{•+} (the C–S BFDE for 3^{•+} was reported in a previous paper).⁸ These values were estimated using the C–S BDEs for the neutral aryl *tert*-butyl sulfoxides **1**, **2**, and **4** and were obtained by DFT calculations carried out using the Gaussian 03 package²² at the B3P86/6-311+G(d,p)//B3P86/6-311+G(d,p) level of theory. The B3P86 functional was chosen because it is reported to be applied with reasonable success to the calculations of BDE values for a variety of C–X bonds,^{23,24} including C–S bonds.^{24–27} The calculated C–S BDEs of **1**, **2**, and **4**²⁸ are reported in Table 2 with the BDFEs of the corresponding radical cations. C–S BDFEs were calculated in CH₃CN using the thermochemical cycle reported in Figure 2, the C–S BDEs for the neutral sulfides corrected for the entropic factor, the peak oxidation potentials of the sulfides reported in Table S1 in the Supporting Information, and the reduction potential of the leaving *tert*-butyl cation (0.09 V vs SCE) available from the literature.²⁹

Because we are dealing with conformationally flexible molecules, before starting the BDE calculations, all the available conformations for the molecule and the radicals formed in the C–S scission process have to be found. To this end, a

Table 2. Maximum Absorption Wavelengths (λ_{max}), Decay Rate Constants (*k_f*) of Aryl *tert*-Butyl Sulfoxide Radical Cations (1^{•+}–4^{•+}) Generated by Photooxidation of 1–4 Sensitized by 3-CN-NMQ⁺ (λ_{exc} = 355 nm), C–S Bond Dissociation Energies (BDEs) for the Aryl *tert*-Butyl Sulfoxides 1–4, and C–S Bond Dissociation Free Energies (BDFEs) for Radical Cations 1^{•+}–4^{•+}

4-XC ₆ H ₄ SOC(CH ₃) ₃	λ _{max} (nm) ^a	<i>k_f</i> (10 ⁵ s ⁻¹) ^a	C–S BDE (neutral substrates) ^{b,c}	C–S BDFE (radical cations) ^{c,d,e}
1 ^{•+} X = MeO	620	1.9 ± 0.5	35.80	–12.5
2 ^{•+} X = Me	570	4.1 ± 0.5	35.94	–16.9
3 ^{•+} X = H	520 ^f	14 ^f	36.2 ^f	–18.1 ^f
4 ^{•+} X = Br	590	18 ± 2	36.39	–19.9

^aFrom LFP experiments in N₂-saturated CH₃CN. [Sulfide] = 1.0 × 10⁻² M; [3-CN-NMQ⁺] = 8 × 10⁻⁴ M. ^bFrom DFT calculations; see text. ^cIn kilocalories per mole. ^dAt 298 K. ^eDetails of calculations in the Supporting Information. ^fFrom ref 8.

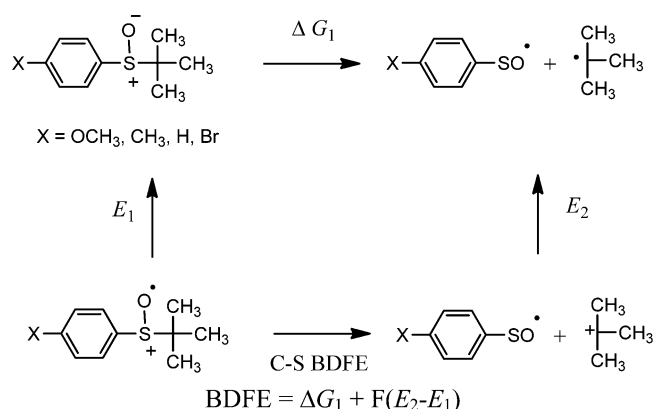


Figure 2. Thermochemical cycle for the calculation of C–S BDFE values of sulfoxide radical cations $1^{+\bullet}$ – $4^{+\bullet}$.

systematic conformational search was carried out, at the semiempirical PM3 level of theory,³⁰ using the Conformer Search Module available in the Spartan 5.01 package.³¹ All the conformers found were optimized again, first at the B3LYP/6-31G level of theory, and then at the higher B3P86/6-311+G(d,p) level of theory. The numbers of conformers found for sulfoxides were two for **1**, two for **2**, and one for **4**. The numbers of conformers found for the arylsulfinyl radicals were two for 4-MeOC₆H₄SO[•], two for 4-MeC₆H₄SO[•], and one for 4-BrC₆H₄SO[•].

In all the calculations, the keywords integral(grid=ultrafine) scf=tight were used. For open shell (radical) species, spin contamination due to states of multiplicity higher than the doublet state was negligible because the expectation value $\langle S^2 \rangle$ of the total spin operator S^2 was, in all cases, within 5% of the expectation value for a doublet (0.75). Harmonic vibrational frequencies were calculated at the B3P86/6-311+G(d,p) level of theory to confirm that the stationary points found correspond to local minima and to obtain the zero-point vibrational energy (ZPVE) corrections. For the ZPVE, a scale factor of 0.9845 was used.³² When more than one conformer was found for a given compound, its energy ($E_{\text{el}} + E_{\text{ZPVE}}$) to be used in the BDE calculation was obtained by Boltzmann averaging the energy ($E_{\text{el}} + E_{\text{ZPVE}}$) of all the corresponding minima. In the Supporting Information are reported the Cartesian coordinates, the electronic energy, and the zero-point vibrational energy of all the minima found.

Sulfoxide Radical Cations. DFT calculations were performed for sulfoxide radical cations $1^{+\bullet}$ – $4^{+\bullet}$ with the aim of obtaining the geometry of the minima, charges, and spin distributions. The calculations were carried out at the B3LYP/6-311G(d,p)//B3LYP/6-311G(d,p) level of theory, the same that was used in previous works on aryl sulfide radical cations.^{13,33}

The starting geometries for the energy minimization of each radical cation were those of the corresponding neutral sulfoxide. Harmonic vibrational frequencies were calculated at the B3LYP/6-311G(d,p) level of theory to confirm that the stationary points found correspond to local minima. For all the radical cations, spin contamination due to states of multiplicity higher than the doublet state was negligible because the expectation value $\langle S^2 \rangle$ of the total spin operator S^2 was, in all cases, within 5% of the expectation value for a doublet (0.75). The number of conformers found for sulfoxide radical cations $1^{+\bullet}$ – $4^{+\bullet}$ were two for $1^{+\bullet}$, two for $2^{+\bullet}$, one for $3^{+\bullet}$, and one for $4^{+\bullet}$. The atomic charges were obtained by

natural population analysis (NPA).³⁴ Unpaired electron spin densities were calculated using the Mulliken population analysis.

The two energy minimum conformations for $1^{+\bullet}$ and $2^{+\bullet}$ differ only for the dihedral angle of the substituent and have very similar energies: $1a^{+\bullet}$ is 0.14 kcal/mol lower in energy than $1b^{+\bullet}$, whereas $2a^{+\bullet}$ is 0.04 kcal/mol lower in energy than $2b^{+\bullet}$.

In Figure 3 are displayed the two most stable conformers of $1^{+\bullet}$. Energy minimum conformations for $2^{+\bullet}$, $3^{+\bullet}$, and $4^{+\bullet}$ are reported in Figures S7 and S8 in the Supporting Information.

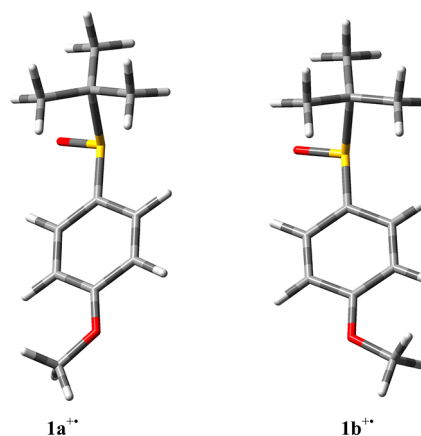


Figure 3. Most stable conformers for 4-MeOC₆H₄SOC(CH₃)₃^{+\bullet} ($1^{+\bullet}$).

In Table 3 are displayed NPA charges and spin density values obtained for the conformers of radical cations $1^{+\bullet}$ – $4^{+\bullet}$,

Table 3. NPA Charges (q_{NPA}) and Spin Densities for Radical Cations $1^{+\bullet}$ – $4^{+\bullet}$

		X	Ar	S	O	tert-butyl
$1a^{+\bullet}$	q_{NPA}	−0.078	0.314	1.275	−0.747	0.236
$1a^{+\bullet}$	spin	0.080	0.238	0.191	0.297	0.194
$1b^{+\bullet}$	q_{NPA}	−0.078	0.314	1.274	−0.744	0.234
$1b^{+\bullet}$	spin	0.081	0.236	0.189	0.301	0.194
$2a^{+\bullet}$	q_{NPA}	0.087	0.027	1.231	−0.701	0.355
$2a^{+\bullet}$	spin	0.007	0.158	0.219	0.372	0.244
$2b^{+\bullet}$	q_{NPA}	0.087	0.029	1.236	−0.700	0.349
$2b^{+\bullet}$	spin	0.007	0.160	0.220	0.373	0.240
$3^{+\bullet}$	q_{NPA}	–	0.049	1.139	−0.698	0.510
$3^{+\bullet}$	spin	–	0.104	0.230	0.384	0.282
$4^{+\bullet}$	q_{NPA}	0.189	−0.102	1.157	−0.713	0.471
$4^{+\bullet}$	spin	0.038	0.117	0.209	0.353	0.283

partitioned for the different structural components of the radical cations defined in Figure 4.

In the attempt to identify a possible transition state for the C–S bond cleavage in the radical cations, we stepwise elongated the C–S bond in the radical cations $1^{+\bullet}$ – $4^{+\bullet}$ starting

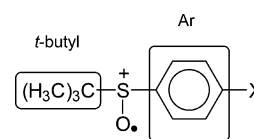


Figure 4. Structural components of aryl tert-butyl sulfoxide radical cations.

from the energy minimum conformations. For radical cations $1^{+\bullet}$ and $2^{+\bullet}$, the most stable conformer was chosen. We partially optimized the geometry for each bond length. In the optimization process, the C–S bond length was kept fixed, whereas all the other degrees of freedom were allowed to relax. By increasing the C–S bond, we observed an initial increase of the energy of the system followed by a decrease at longer C–S distances (Figure 5).

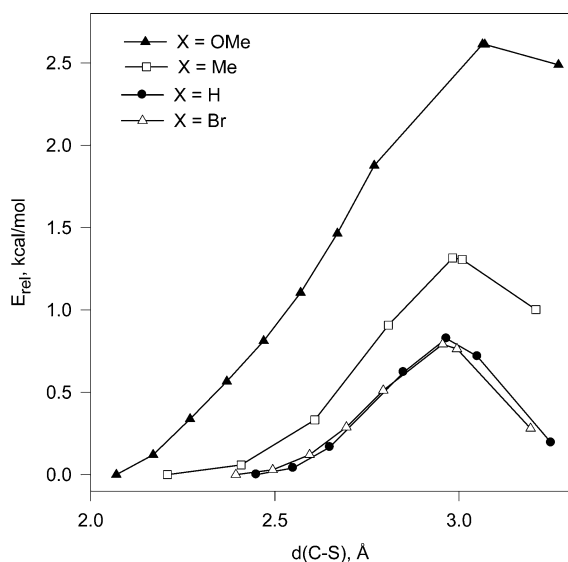


Figure 5. Plot of E_{rel} vs the C–S bond distances ($d(C-S)$) for radical cations $1^{+\bullet}$ (\blacktriangle), $2^{+\bullet}$ (\square), $3^{+\bullet}$ (\bullet), and $4^{+\bullet}$ (\triangle).

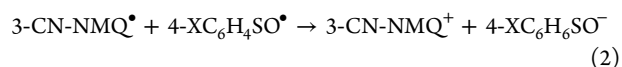
For each radical cation, the geometry corresponding to the maximum energy value was optimized (opt=TS) to the nearest transition state. Each stationary point found was characterized by a frequency calculation, and one imaginary frequency was found, thus confirming that the stationary point found is a saddle point. Furthermore, the normal mode corresponding to the imaginary frequency was animated using the visualization program Molden.³⁵ In this way it was verified that the displacements composing the mode correspond to the C–S bond fragmentation process.

In Table 4 are displayed the C–S bond distances, the relative energies of the transition states, the NPA charges (q_{NPA}), and spin density values obtained for the optimized structures of radical cations $1^{+\bullet}$ – $4^{+\bullet}$ and for the TS, partitioned for the different structural components defined in Figure 4.

DISCUSSION

The results of the steady-state photolysis experiments supported the existence of a heterolytic C–S bond cleavage in aryl *tert*-butyl sulfoxide radical cations $1^{+\bullet}$ – $4^{+\bullet}$. In all cases, *tert*-butyl acetamide and *tert*-butyl alcohol are formed as the primary reaction products from the *tert*-butyl cation, produced by the C–S bond cleavage, which reacts with the solvent (Ritter reaction) or adventitious water (Scheme 2).

The sulfur-containing products (diaryl disulfide (ArSSAr), aryl arenethiosulfinate (ArSOSAr), and aryl arenethiosulfonate (ArSO₂SAr)) derive instead from the arylsulfinyl radical. Dimerization of ArSO[•] might lead to the aryl arenethiosulfonates.^{7,36} Diaryl disulfides and aryl arenethiosulfonates likely derive from the aryl sulfenates formed after reduction of ArSO[•] by 3-CN-NMQ[•] (eq 2). This exergonic process⁸ can explain the observation that 3-CN-NMQ⁺ is not entirely consumed during the irradiation.



From the sulfenate anion or its protonated sulfenic acid form, ArSOSAr and ArSSAr can be produced according to the reactions displayed in Scheme 3. Small amounts of aryl sulfinic acids that might get lost during workup can also be formed. This can explain the slightly lower overall quantum yield of sulfur-containing products as compared to that of the products from the *tert*-butyl moiety.

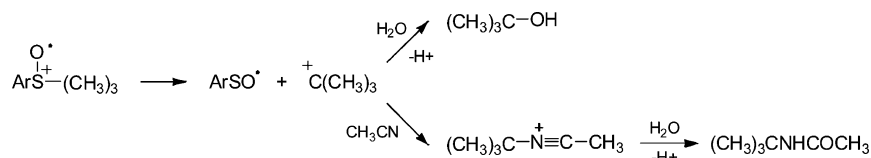
The kinetic analysis of the C–S bond fragmentation in aryl *tert*-butyl sulfoxide radical cations $1^{+\bullet}$ – $4^{+\bullet}$, carried out by LFP experiments in CH₃CN following the unimolecular decay of the radical cations at their maximum absorption wavelengths, has provided important information on the quantitative aspects of the electronic effects of arylsulfinyl ring substituents on C–S bond cleavage. From the fragmentation rate constants (k_f) of $1^{+\bullet}$ – $4^{+\bullet}$ reported in Table 2, it can be immediately noted that, as expected, the rates increase by decreasing the electron donating power of the substituent, that is by decreasing the stability of the radical cations. However, the substituent effect on the C–S bond cleavage rates is rather small because an increase in the fragmentation rate of less than 10 times is observed when going from the most stable 4-MeO-substituted radical cation $1^{+\bullet}$ to the less stable 4-Br-substituted radical cation $4^{+\bullet}$. The 7.4 kcal/mol difference in BDFE between $1^{+\bullet}$ and $4^{+\bullet}$ (Table 2) is associated with a very small difference in ΔG^{\ddagger} (1.4 kcal/mol).

Theoretical calculations have been carried out in order to have information on the energetics of the C–S bond cleavage

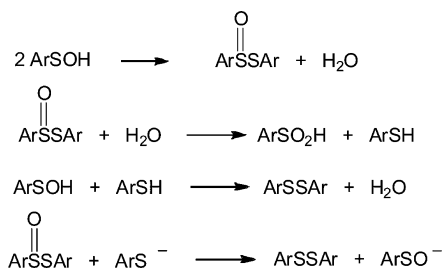
Table 4. C–S Bond Distances ($d(C-S)$), Relative Energies (E_{rel}) of the Transition States (TS) for the C–S Bond Fragmentation Process in Radical Cations $1^{+\bullet}$ – $4^{+\bullet}$, NPA Charges (q_{NPA}), and Spin Densities for Radical Cations $1^{+\bullet}$ – $4^{+\bullet}$ and for the Corresponding Transition States

	$d(C-S)$ (Å)	E_{rel} (kcal/mol)	q_{NPA}				spin			
			X	Ar	SO	<i>t</i> -Bu	X	Ar	SO	<i>t</i> -Bu
$1^{+\bullet}$	2.070	0	−0.078	0.314	0.528	0.236	0.080	0.238	0.488	0.194
$1^{+\bullet}$ (TS)	3.064	2.61	−0.112	0.223	0.208	0.681	0.045	0.150	0.539	0.266
$2^{+\bullet}$	2.209	0	0.087	0.027	0.530	0.355	0.007	0.158	0.591	0.244
$2^{+\bullet}$ (TS)	2.983	1.32	0.078	−0.028	0.250	0.700	0.004	0.128	0.616	0.252
$3^{+\bullet}$	2.450	0	–	0.049	0.441	0.510	–	0.104	0.614	0.282
$3^{+\bullet}$ (TS)	2.966	0.827	–	0.017	0.260	0.723	–	0.109	0.662	0.229
$4^{+\bullet}$	2.394	0	0.188	−0.102	0.443	0.471	0.038	0.117	0.562	0.283
$4^{+\bullet}$ (TS)	2.956	0.792	0.168	−0.131	0.253	0.710	0.024	0.108	0.630	0.238

Scheme 2



Scheme 3



in aryl sulfoxide radical cations $1^{\bullet+}$ – $4^{\bullet+}$ and to provide a possible explanation of the relatively small substituent effects on the C–S fragmentation rate constants. DFT calculations for $1^{\bullet+}$ and $2^{\bullet+}$ indicated the presence of two energy minimum conformations very similar from both geometric and energetic points of view, whereas only one conformer at the minimum energy was found for $3^{\bullet+}$ and $4^{\bullet+}$. As shown in Figure 3 and Figures S7 and S8 in the Supporting Information, the *tert*-butyl group is almost perpendicular to the arylsulfanyl ring as observed in our previous study of the most stable conformations of aryl methyl sulfoxide radical cations.⁵

The NPA charges and spin populations in $1^{\bullet+}$ – $4^{\bullet+}$ (Table 3) are mainly localized on the sulfinyl group. The charge and spin density are also relatively high on the *tert*-butyl group and decrease by increasing the electron donating power of the X substituent.

The increase of the C–S bond distance starting from the energy minimum conformations led to an initial increase in the energy of the system followed by a decrease at longer C–S distances (Figure 5). Thus, the transition states for the C–S fragmentation process have been identified. As predicted for the highly exergonic C–S bond cleavage processes, the TS are reached quite early along the reaction coordinate, and a relatively small increase of the C–S bond distance is observed.

If we compare the TS of the C–S fragmentation of aryl *tert*-butyl sulfoxide radical cations, it can be noted that the C–S bond distance and the energy relative to the starting conformer (E_{rel}) increase regularly by increasing the electron releasing power of the substituent (Table 4). The increase of the C–S bond distance in the TS and the degree of elongation of the C–S bond as measured by the increase of the C–S bond in the TS (ca. 23% of the initial bond length for $4^{\bullet+}$ and ca. 48% for $1^{\bullet+}$) with the electron donating power of the substituents reflect a later TS for the less exergonic processes. The highest and lowest E_{rel} values, found for $1^{\bullet+}$ and $4^{\bullet+}$, respectively, are in accordance with the lowest and highest rate of C–S fragmentation found for these radical cations.

It is interesting to note that the electronic effects of the X substituent on the C–S bond cleavage in aryl *tert*-butyl sulfoxide radical cations are significantly lower than those observed in the C–S fragmentation of aryl triphenylmethyl sulfide radical cation, where the C–S bond cleavage rates were very sensitive to the nature of the substituent.¹³ A possible

explanation of this fact can be based on the results of DFT calculations showing that a significant fraction of the charge is delocalized in the *tert*-butyl group of the radical cations. Such a delocalization is probably at the origin of the observation that rates of C–S bond cleavage showed little sensitivity to changes in the C–S bond dissociation free energy (BDFE). On the contrary, for aryl triphenylmethyl sulfide radical cations, the same type of calculations indicated that most of the charge is localized in the ArS moiety of the radical cation and a significant delocalization of the charge and spin density when going from the reactant to the TS of the C–S fragmentation process should occur, explaining the greater substituent effects on the C–S bond cleavage rates.

In our previous studies,⁸ we have suggested that the C–S bond cleavage in aryl sulfoxide radical cations should be characterized by a relatively high reorganization energy (λ). In particular, the λ value for the fragmentation process should be significantly larger for aromatic sulfoxide than for aromatic sulfide radical cations. This hypothesis can account for the fact that the difference in fragmentation rates between sulfide and sulfoxide radical cations (at least 2 orders of magnitude) appears small relative to the difference in the thermodynamic driving force.^{8,10,37}

In order to verify our hypothesis, we have treated the kinetic data for the fragmentation of radical cations $1^{\bullet+}$ – $4^{\bullet+}$ in terms of the Marcus equation (eq 3),³⁸ where ΔG^\ddagger is the activation free energy of the reaction calculated by the Eyring equation (eq 4), replacing k_f with the values reported in Table 2, and Z as $6 \times 10^{11} \text{ M}^{-1} \text{ s}^{-1}$.³⁹ ΔG° is the free-energy variation in the same reaction (C–S BDFE given in Table 2), and λ is the reorganization energy required for the fragmentation process.

$$\Delta G^\ddagger = (\lambda/4)(1 + \Delta G^\circ/\lambda)^2 \quad (3)$$

$$\Delta G^\ddagger = RT \ln(Z/k_f) \quad (4)$$

A good fit of the experimental data to eq 3 was obtained and is shown in Figure 6. The λ value obtained from the nonlinear least-squares fitting of the data (62 kcal/mol) clearly indicates a quite high intrinsic barrier for the C–S bond cleavage reaction.

The very high λ value obtained from the Marcus plot confirms our hypothesis, clearly indicating that a large reorganization energy is an intrinsic characteristic of the C–S bond fragmentation process of aryl sulfoxide radical cations. It has to be noted that the λ value is even higher than those previously determined for the C–S bond cleavage in aryl triphenylmethyl sulfide¹³ and aryl cumyl sulfide radical cations³³ (ca. 52 and 44 kcal mol⁻¹, respectively).

As proposed in the previous study,⁸ the higher λ value for the C–S bond cleavage in aryl sulfoxide radical cations might be associated with the presence of the very polar S–O bond that is well-solvated in CH₃CN. The quite large internal and solvent reorganization energies mainly derive from the change in the length and polarity of the S–O bond during the fragmentation process. Accordingly, when going from the starting sulfoxide radical cations $1^{\bullet+}$ – $4^{\bullet+}$ to the TS of the C–S fragmentation

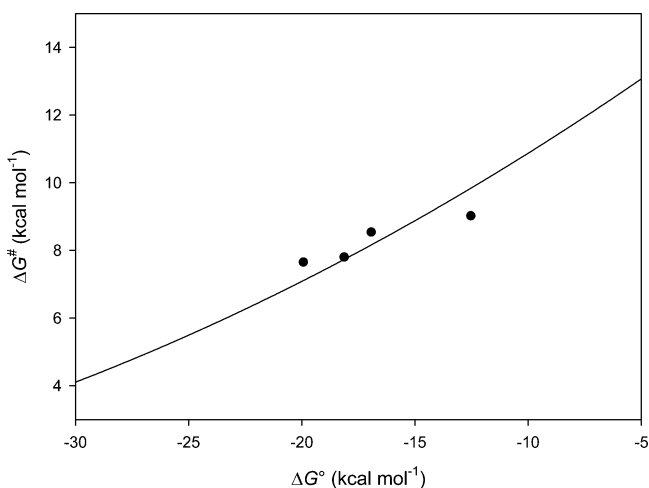


Figure 6. Diagram of ΔG^\ddagger vs ΔG° for the fragmentation reactions of radical cations $1^{\bullet+}$ – $4^{\bullet+}$. The solid circles correspond to the experimental values; the curve is calculated by a nonlinear least-squares fit to eq 3.

process, we observe an increase of the negative charge on oxygen and a decrease of the positive charge on sulfur in addition to an increase of the S–O bond length (see Table S2 in the Supporting Information).

CONCLUSIONS

The C–S bond cleavage rates in aryl *tert*-butyl sulfoxide radical cations show little sensitivity to the nature of the substituent, decreasing by increasing the electron donating properties of the arylsulfenyl ring substituent, that is by increasing the stability of the radical cations. These results have been explained by considering that a significant fraction of the charge and spin densities are delocalized in the *tert*-butyl group of the radical cations, and little further accumulation of the charge and spin density should occur when going from the reactant to the TS of the C–S fragmentation process. A different situation was observed in a previous study for the C–S fragmentation of aryl triphenylmethyl sulfide radical cations¹³ where most of the charge is localized in the ArS moiety and the aryl substituents exerted a significant effect on the C–S bond cleavage rates.

C–S bond cleavage in aryl sulfoxide radical cations is characterized by a particularly high reorganization energy (λ), much higher than that found in the C–S fragmentation process of aromatic sulfide radical cations, most likely because of the presence of the very polar S–O bond that is well solvated in CH_3CN .

EXPERIMENTAL SECTION

Starting Materials. *tert*-Butyl phenyl sulfoxide (**3**) was synthesized and characterized in a previous study.⁸ *tert*-Butyl 4-methoxyphenyl sulfoxide (**1**), *tert*-butyl 4-methylphenyl sulfoxide (**2**), and 4-bromophenyl *tert*-butyl sulfoxide (**4**) were prepared by oxidation of the corresponding sulfides with sodium periodate in aqueous ethanol⁴⁰ as previously reported for the synthesis of **3**. *tert*-Butyl 4-methoxyphenyl sulfide, *tert*-butyl 4-methylphenyl sulfide, and 4-bromophenyl *tert*-butyl sulfide were prepared by acid-catalyzed reaction of the corresponding thiophenols with *tert*-butyl alcohol.⁴¹ 3-Cyano-*N*-methylquinolinium perchlorate was prepared by reaction of 3-cyanoquinoline with dimethyl sulfate; the sulfate salt was then transformed to the perchlorate salt using perchloric acid.⁴² *tert*-Butylacetamide, aryl arylthiosulfonates were prepared according to literature procedures.^{43,44} Aryl arylthiosulfonates were prepared by

oxidation of diaryl disulfides with the $\text{H}_2\text{O}_2/\text{MoO}_2\text{Cl}_2$ system in CH_3CN at room temperature.⁴⁵ Aryl *tert*-butyl sulfones were synthesized by oxidation of the corresponding sulfides with H_2O_2 in glacial acetic acid.⁴⁶ CH_3CN (spectrophotometric grade) was distilled over CaH_2 .

Spectral data of substrates **1** and **2** and of reaction products are in accordance with those reported in the literature.^{47,48}

4-Bromophenyl *tert*-Butyl Sulfoxide (4**).** To a solution of 4-bromophenyl *tert*-butyl sulfide⁴¹ (1.03 g, 4.2 mmol) in 150 mL of methanol/water (1:1) was added sodium periodate (0.9 g, 4.2 mmol), and the reaction mixture was stirred overnight at room temperature and then extracted with chloroform. The extract was dried over anhydrous magnesium sulfate, and the solvent was removed under reduced pressure. **4** was purified by column chromatography (hexane/ethyl acetate, 3:1) and obtained as a white solid (0.6 g, 55%): mp 70–72 °C; ¹H NMR (300 MHz, CD_3CN) δ 1.08 (s, 9H), 7.46–7.69 (m, 4H); ¹³C NMR (300 MHz, CD_3CN) δ 21.5, 55.1, 124.6, 127.6, 131.2, 139.6; HRMS (ESI-TOF) calcd for $\text{C}_{10}\text{H}_{13}\text{SOBr} + \text{Na}^+$ 282.9768, found 282.9812.

Steady-State Photolysis. A 1 mL solution containing 3-CN-NMQ⁺ (1.0×10^{-3} M) and **1–4** (1.0×10^{-2} M) in N_2 -saturated CD_3CN placed in a Schlenk tube was irradiated with four phosphor-coated fluorescent lamps emitting at 355 ± 15 nm. An internal standard (methyl phenyl sulfoxide) was added, and the mixtures were analyzed by ¹H NMR and HPLC. The following products were identified by comparison with authentic specimens: *tert*-butyl alcohol, *tert*-butyl acetamide, diaryl disulfides, aryl arylthiosulfonates, aryl arylthiosulfonates, and aryl *tert*-butyl sulfones. The photoproducts were quantified by HPLC and ¹H NMR. HPLC was performed with an HP Agilent 1100 Series HPLC system with a UV/visible detector at 230 nm. An Alltima C18 column (5 μm , 4.6×250 mm) was equilibrated with $\text{CH}_3\text{OH}/\text{H}_2\text{O}$ (75:25), and compounds were eluted with an ascending gradient of CH_3OH (75–100%) at a flow rate of 0.7 mL/min. The material balance was always satisfactory (>90%). A blank experiment, carried out by irradiating the solutions in the absence of 3-CN-NMQ⁺ ClO_4^- , did not show in any case product formation.

Laser Flash Photolysis. An excitation wavelength of 355 nm (Nd:YAG laser, Continuum, third harmonic, pulse width ca. 7 ns and energy <3 mJ per pulse) was used in nanosecond flash photolysis experiments. A 1 mL solution containing the substrate (1.0×10^{-2} M), the sensitizer (3-CN-NMQ⁺, 8.8×10^{-4} M), and the cosensitizer (1 M toluene) was flashed in a quartz photolysis cell while nitrogen was bubbling through them. All measurements were carried out at 22 ± 2 °C. The transient spectra were obtained by a point-to-point technique, monitoring the change of absorbance (ΔA) after the laser flash at intervals of 5–10 nm over the spectral range of 350–700 nm, averaging at least 10 decays at each wavelength. The error estimated on the rate constants was $\pm 10\%$.

Theoretical Calculations. The calculations were run on the 22TFlops Linux Cluster “Matrix” consisting of 330 nodes dual-socket quad-core Opteron CPU each with Infiniband DDR as the main interconnect and a shared filesystem based on Lustre 1.8.4 via IB. Located at Rome supercomputing center CASPUR.

ASSOCIATED CONTENT

Supporting Information

¹H NMR and ¹³C NMR spectra of 4-Br-C₆H₄SOC(CH₃)₃ (**4**); ¹H NMR spectrum and HPLC chromatogram of the 3-CN-NMQ⁺ photosensitized oxidation of *tert*-butyl 4-methoxyphenyl sulfoxide (**1**); time-resolved absorption spectra after LFP of the 3-CN-NMQ⁺/toluene/2 and 3-CN-NMQ⁺/toluene/4 systems in CH_3CN ; cyclic voltammetry; C–S BDFEs of radical cations $1^{\bullet+}$ – $4^{\bullet+}$, conformers at the minimum of energy of $2^{\bullet+}$, $3^{\bullet+}$, and $4^{\bullet+}$; Cartesian coordinates, energies, and ZPVE from DFT calculations for neutral sulfides **1**, **2**, and **4**, for arylsulfenyl radicals, and for radical cations $1^{\bullet+}$ – $4^{\bullet+}$; Cartesian coordinates and energies for TS of the C–S bond cleavage in the radical cations $1^{\bullet+}$ – $4^{\bullet+}$; and S–O bond distances and NPA charges on

sulfur and oxygen in radical cations $1^{+\bullet}$ – $4^{+\bullet}$ and in the TS for the C–S bond fragmentation process. This material is available free of charge via the Internet at <http://pubs.acs.org>.

AUTHOR INFORMATION

Corresponding Author

*O.L.: osvaldo.lanzalunga@uniroma1.it. T.D.: dgiacco@uniupg.it. P.M.: paolo.mencarelli@uniroma1.it.

Notes

The authors declare no competing financial interest.

ACKNOWLEDGMENTS

Thanks are due to the Ministero dell'Istruzione, dell'Università e della Ricerca (MIUR) for financial support, PRIN 2010-2011 (2010PFLRJR) project (PROxi project). We also thank Prof. Enrico Baciocchi for helpful discussion.

REFERENCES

- (1) Carreno, M. C. *Chem. Rev.* **1995**, *95*, 1717–1760. Fernandez, I.; Khair, N. *Chem. Rev.* **2003**, *103*, 3651–3705.
- (2) Clarke, M. J.; Zhu, F.; Frasca, D. R. *Chem. Rev.* **1999**, *99*, 2511. Lipponer, K. G.; Vogel, E.; Keppler, B. K. *Met.-Based Drugs* **1996**, *3*, 243. Caligaris, M.; Carugo, O. *Coord. Chem. Rev.* **1996**, *153*, 83. Shin, J. M.; Cho, Y. M.; Sachs, G. *J. Am. Chem. Soc.* **2004**, *126*, 7800–7811. Legros, J.; Dehli, J. R.; Bolm, C. *Adv. Synth. Catal.* **2005**, *347*, 19–31. Bentley, R. *Chem. Soc. Rev.* **2005**, *34*, 309–324.
- (3) Charlesworth, P.; Lee, W.; Jenks, W. S. *J. Phys. Chem.* **1996**, *100*, 15152–15155.
- (4) Carlsen, L.; Egsgaard, H. *J. Am. Chem. Soc.* **1988**, *110*, 6701–6705. Kishore, K.; Asmus, K.-D. *J. Phys. Chem.* **1991**, *95*, 7233–7239. Adaikalasamy, K.; Venkataramanan, N. S.; Rajagopal, S. *Tetrahedron* **2003**, *59*, 3613–3619. Ganesan, M.; Sivasubramanian, V. K.; Rajagopal, S.; Ramaraj, R. *Tetrahedron* **2004**, *60*, 1921–1929.
- (5) Baciocchi, E.; Del Giacco, T.; Gerini, M. F.; Lanzalunga, O. *J. Phys. Chem. A* **2006**, *110*, 9940–9948.
- (6) Aurisicchio, C.; Baciocchi, E.; Gerini, M. F.; Lanzalunga, O. *Org. Lett.* **2007**, *9*, 1939–1942.
- (7) Baciocchi, E.; Lanzalunga, O.; Lapi, A.; Maggini, L. *J. Org. Chem.* **2009**, *74*, 1805–1808.
- (8) Baciocchi, E.; Del Giacco, T.; Lanzalunga, O.; Mencarelli, P.; Procacci, B. *J. Org. Chem.* **2008**, *73*, 5675–5682.
- (9) (a) Lanzalunga, O. *Phosphorus, Sulfur Silicon Relat. Elem.* **2013**, DOI: 10.1080/10426507.2012.736108. (b) Lanzalunga, O.; Lapi, A. *J. Sulfur Chem.* **2011**, *33*, 101–129. (c) Baciocchi, E.; Bietti, M.; Lanzalunga, O. *J. Phys. Org. Chem.* **2006**, *19*, 467–478. (d) Peñeñory, A. B.; Argüello, J. E.; Puiatti, M. *Eur. J. Org. Chem.* **2005**, *10*, 114–122. (e) Baciocchi, E.; Bietti, M.; Lanzalunga, O. *Acc. Chem. Res.* **2000**, *33*, 243–251. (f) Glass, R. S. *Top. Curr. Chem.* **1999**, *205*, 1. (g) Adam, W.; Argüello, J. E.; Peñeñory, A. B. *J. Org. Chem.* **1998**, *63*, 3905–3910. (h) Ioele, M.; Steenken, S.; Baciocchi, E. *J. Phys. Chem. A* **1997**, *101*, 2979–2987. (i) Baciocchi, E.; Lanzalunga, O.; Malandrucchio, S.; Ioele, M.; Steenken, S. *J. Am. Chem. Soc.* **1996**, *118*, 8973–8974. (j) Baciocchi, E.; Rol, C.; Scamosci, E.; Sebastiani, G. V. *J. Org. Chem.* **1991**, *56*, 5498–5502.
- (10) Baciocchi, E.; Del Giacco, T.; Gerini, M. F.; Lanzalunga, O. *Org. Lett.* **2006**, *8*, 641–644.
- (11) Baciocchi, E.; Intini, D.; Piermattei, C.; Rol, C.; Ruzziconi, R. *Gazz. Chim. Ital.* **1989**, *119*, 649–652.
- (12) Kice, J. L. In *Free Radicals*; Kochi, J. K., Ed.; John Wiley & Sons: New York, 1973; Chapter 24.
- (13) Del Giacco, T.; Lanzalunga, O.; Mazzonna, M.; Mencarelli, P. *J. Org. Chem.* **2012**, *77*, 1843–1852.
- (14) Baciocchi, E.; Gerini, M. F. *J. Phys. Chem. A* **2004**, *108*, 2332–2338.
- (15) Kitaguchi, H.; Ohkubo, K.; Ogo, S.; Fukuzumi, S. *J. Phys. Chem. A* **2006**, *110*, 1718–1725.
- (16) Formation of aryl *tert*-butyl sulfones (<5% referred to the starting material) probably derives from the presence of traces of oxygen in the reaction mixture. Accordingly, their amounts are significantly reduced by a more extended nitrogen saturation of the reaction mixtures. Aryl sulfones are likely formed by reaction of the sulfoxide radical cations $1^{+\bullet}$ – $4^{+\bullet}$ with superoxide anion produced after reduction of oxygen by the radical 3-CN-NMQ $^{\bullet}$.
- (17) Dockery, K. P.; Dinnocenzo, J. P.; Farid, S.; Goodman, J. L.; Gould, I. R.; Todd, W. P. *J. Am. Chem. Soc.* **1997**, *119*, 1876–1883.
- (18) Schlesener, C. J.; Amatore, C.; Kochi, J. K. *J. Phys. Chem.* **1986**, *90*, 3747–3756.
- (19) Darmanyan, A. P.; Gregory, D. D.; Guo, Y.; Jencks, W. S. *J. Phys. Chem. A* **1997**, *101*, 6855–6863.
- (20) The rate of the self-recombination reaction for PhSO $^{\bullet}$ is $k = 3.0 \times 10^9 \text{ M}^{-1} \text{ s}^{-1}$.¹⁹
- (21) Baciocchi, E.; Del Giacco, T.; Giombolini, P.; Lanzalunga, O. *Tetrahedron* **2006**, *62*, 6566–6573.
- (22) Frisch, M. J.; Trucks, G. W.; Schlegel, H. B.; Scuseria, G. E.; Robb, M. A.; Cheeseman, J. R.; Montgomery, J. A., Jr.; Vreven, T.; Kudin, K. N.; Burant, J. C.; Millam, J. M.; Iyengar, S. S.; Tomasi, J.; Barone, V.; Mennucci, B.; Cossi, M.; Scalmani, G.; Rega, N.; Petersson, G. A.; Nakatsuji, H.; Hada, M.; Ehara, M.; Toyota, K.; Fukuda, R.; Hasegawa, J.; Ishida, M.; Nakajima, T.; Honda, Y.; Kitao, O.; Nakai, H.; Klene, M.; Li, X.; Knox, J. E.; Hratchian, H. P.; Cross, J. B.; Adamo, C.; Jaramillo, J.; Gomperts, R.; Stratmann, R. E.; Yazyev, O.; Austin, A. J.; Cammi, R.; Pomelli, C.; Ochterski, J. W.; Ayala, P. Y.; Morokuma, K.; Voth, G. A.; Salvador, P.; Dannenberg, J. J.; Zakrzewski, V. G.; Dapprich, S.; Daniels, A. D.; Strain, M. C.; Farkas, O.; Malick, D. K.; Rabuck, A. D.; Raghavachari, K.; Foresman, J. B.; Ortiz, J. V.; Cui, Q.; Baboul, A. G.; Clifford, S.; Cioslowski, J.; Stefanov, B. B.; Liu, G.; Liashenko, A.; Piskorz, P.; Komaromi, I.; Martin, R. L.; Fox, D. J.; Keith, T.; Al-Laham, M. A.; Peng, C. Y.; Nanayakkara, A.; Challacombe, M.; Gill, P. M. W.; Johnson, B.; Chen, W.; Wong, M. W.; Gonzalez, C.; Pople, J. A. *Gaussian 03*, revision B.05; Gaussian, Inc.: Pittsburgh, PA, 2003.
- (23) (a) Yao, X.-Q.; Hou, X.-J.; Jiao, H.; Wu, G.-S.; Xu, Y.-Y.; Xiang, H.-W.; Jiao, H.; Li, Y.-W. *J. Phys. Chem. A* **2002**, *106*, 7184–7189. (b) Zhao, J.; Cheng, X.; Yang, X. *J. Mol. Struct.: THEOCHEM* **2006**, *766*, 87–92. (c) Van Speybroeck, V.; Marin, G. B.; Waroquier, M. *Chem. Phys. Chem.* **2006**, *7*, 2205–2214. (d) Su, X.-F.; Cheng, X.; Liu, Y.-G.; Li, Q. *Int. J. Quantum Chem.* **2007**, *107*, 515–521.
- (24) (a) Johnson, E. R.; Clarkin, O. J.; DiLabio, G. A. *J. Phys. Chem. A* **2003**, *107*, 9953–9963. (b) Yao, X.-Q.; Hou, X.-J.; Jiao, H.; Xiang, H.-W.; Li, Y.-W. *J. Phys. Chem. A* **2003**, *107*, 9991–9996. (c) Feng, Y.; Liu, L.; Wang, J.-T.; Huang, H.; Guo, Q.-X. *J. Chem. Inf. Model.* **2003**, *43*, 2005–2013.
- (25) Even though DFT methods may underestimate absolute BDE values,^{24c,26} this should not affect the relative BDE values which are those we are mostly concerned with in this paper.
- (26) The C–S BDE of dimethyl sulfoxide calculated by this method (44.5 kcal mol $^{-1}$) is significantly lower than the experimental BDE value of 53 kcal mol $^{-1}$.²⁷
- (27) Luo, Y.-R. *Comprehensive Handbook of Chemical Bond Energies*; CRC Press: Boca Raton, FL, 2007.
- (28) C–S BDEs are gas-phase values; no significant variation should be expected in the presence of a solvent.
- (29) Wayner, D. D. M.; McPhee, D. J.; Griller, D. *J. Am. Chem. Soc.* **1988**, *110*, 132–137.
- (30) Stewart, J. J. P. *J. Comput. Chem.* **1989**, *10*, 209–220.
- (31) *Spartan 5.01*; Wavefunction, Inc.: Irvine, CA.
- (32) Merrick, J. P.; Moran, D.; Radom, L. *J. Phys. Chem. A* **2007**, *111*, 11683–11700.
- (33) Baciocchi, E.; Bettoni, M.; Del Giacco, T.; Lanzalunga, O.; Mazzonna, M.; Mencarelli, P. *J. Org. Chem.* **2011**, *76*, 573–582.
- (34) Reed, A. E.; Curtiss, L. A.; Weinhold, F. *Chem. Rev.* **1988**, *88*, 899–926.
- (35) Schaftenaar, G.; Noordik, J. H. Molden: a pre- and post-processing program for molecular and electronic structures. *J. Comput.-Aided Mol. Des.* **2000**, *14*, 123.

(36) Chatgililoglu, C. In *The Chemistry of Sulfoxes and Sulfoxides*; Patai, S., Rappoport, Z., Stirling, C. J. M., Eds.; John Wiley & Sons: Chichester, England, 1988; Chapter 24.

(37) This consideration is based on the comparison of the fragmentation rate of *tert*-butyl phenyl sulfoxide radical cation ($3^{+\bullet}$) ($1.4 \times 10^6 \text{ M}^{-1} \text{ s}^{-1}$)⁸ and that of *tert*-butyl phenyl sulfide radical cation that has been estimated as $<10^4 \text{ M}^{-1} \text{ s}^{-1}$.¹⁰ Even though this difference may seem very large, it should be noted that it is associated with a really large change (almost 25 kcal mol^{-1}) in the C–S BDFE for the two radical cations, from $7.6 \text{ kcal mol}^{-1}$ for the sulfide to $-18.1 \text{ kcal mol}^{-1}$ for the sulfoxide.

(38) Marcus, R. A. *Annu. Rev. Phys. Chem.* **1964**, *15*, 155–196.

(39) Ebersson, L. *Electron Transfer Reactions in Organic Chemistry*; Springer Verlag: Berlin, 1986; Chapter 3.

(40) Leonard, N. J.; Johnson, C. R. *J. Org. Chem.* **1962**, *27*, 282–284.

(41) Screttas, C. G.; Micha-Screttas, M. *J. Org. Chem.* **1977**, *42*, 1462–1465. Cutress, N. C.; Grindley, T. B.; Katritzky, A. R.; Topsom, R. D. *J. Chem. Soc., Perkin Trans. 2* **1974**, 263–268.

(42) Kato, S.; Nakata, J.; Imoto, E. *Bull. Chem. Soc. Jpn.* **1971**, *44*, 1928–1933.

(43) Lopez-Serrano, P.; Jongejan, J. A.; Rantwijk, F.; van Sheldon, R. A. *Tetrahedron: Asymmetry* **2001**, *12*, 219–228. Newcomb, M.; Varck, T. R.; Goh, S.-H. *J. Am. Chem. Soc.* **1990**, *112*, 5186–5193.

(44) Kice, J. L.; Rogers, T. E. *J. Am. Chem. Soc.* **1974**, *96*, 8015–8019.

(45) Jeyakumar, K.; Chand, D. K. *Tetrahedron Lett.* **2006**, *47*, 4573–4576.

(46) Iwao, M.; Iihama, T.; Mahalanabis, K. K.; Perrier, H.; Snieckus, V. *J. Org. Chem.* **1989**, *54*, 24–26.

(47) Mohraz, M.; Jian-qi, W.; Heilbronner, E.; Solladie-Cavallo, A.; Matloubi-Moghadam, F. *Helv. Chim. Acta* **1981**, *64*, 97–112. Wang, P.; Chen, J.; Cun, L.; Deng, J.; Zhu, J.; Liao, J. *Org. Biomol. Chem.* **2009**, *7*, 3741–3747.

(48) Abdo, M.; Knapp, S. *J. Org. Chem.* **2012**, *77*, 3433–3438. Bahrami, K.; Khodaei, M. M.; Khaledian, D. *Tetrahedron Lett.* **2012**, *53*, 354–358. Xu, Y.; Peng, Y.; Sun, J.; Chen, J.; Ding, J.; Wu, H. *J. Chem. Res.* **2010**, *6*, 358–360. Lanfranchi, D. A.; Hanquet, G. *J. Org. Chem.* **2006**, *71*, 4854–4861. Clennan, E. L.; Stensaas, K. L. *J. Org. Chem.* **1996**, *61*, 7911–7917. Capozzi, G.; Menichetti, S.; Rosi, A. *J. Chem. Soc., Perkin Trans. 2* **1992**, 2247–2251. Ghersetti, S.; Modena, G. *Spectrochim. Acta* **1963**, *19*, 1809–1810.